

Contents

1	Optimization of peak capacity	3
1.1	Introduction	3
1.2	Theory	5
1.2.1	Peak capacity in isocratic elution	7
1.2.2	Peak capacity in gradient elution	9
1.3	Optimization of peak capacity	11
1.3.1	Optimization of isocratic separations	12
1.3.2	Optimization of gradient separations	23
1.4	Conclusions	30
	References	35

Chapter 1

Optimization of peak capacity

1.1 Introduction

The ultimate goal of analytical liquid chromatography is to provide high separation power in the shortest time possible. In HPLC, performance means peak width. The higher the performance of a chromatographic method, the narrower the peaks are on the chromatogram. Several measures exist for the quantification of quality of a separation or of a chromatogram. The most commonly used one is the number of theoretical plates, N , which is considered as a benchmark measure. The use of plate count, however, has disadvantages. Although it can estimate widths of peaks in isocratic measurements, it cannot be used in gradient separations directly, nor it can tell anything about the overall separation power of the chromatographic method. A column even with the highest plate count ever is useless if all the compounds elute together in a very narrow time range. Resolution, on the other hand, can be used for the characterization of separation quality of neighboring compounds in both isocratic and gradient runs. However, resolution does not serve any information on the general column performance. Peak capacity, a concept introduced by Giddings [1] in 1967, is a very intuitive and at the same time much more general measure than plate count and resolution. Peak capacity is the maximum number of components resolvable by HPLC with a unity resolution [2]. It combines the entire chromatographic space with the variability of the peak widths over the chromatogram. While the number of the actually resolved peaks depends on the nature of solutes existing in a particular mixture, peak capacity can be used to approximate the overall separation power of a given column. Since the introduction of the peak capacity concept, it has been used widely in chromatography both in theoretical studies and method developments.

In method development, peak capacity has a significant importance in analysis of complex samples (e.g. protein tryptic digests). Complete resolution of all components in these samples is often impossible by unidimensional chromatography due to the large number of compounds, even if it is smaller than the peak capacity offered by the method. In that case, the analyst should

focus on decreasing the degree of overlap of the components by maximizing the peak capacity of the system. When simpler mixtures containing much fewer components are analyzed, the optimization of resolutions of pairs of compounds by adjusting the selectivities through the variation of separation conditions is a suitable approach. The effectiveness of this concept, however, is limited as the number of components becomes much larger than 15–20 [3].

Comparison of separations is not always a straightforward task. Giddings introduced [4] the concept of kinetic plots to compare the theoretical limit of separating speed of gas and liquid chromatography by plotting the logarithm of analysis time against the logarithm of plate count. This approach was used and extended by Knox and Saleem [5], and Guiochon [6]. In 1997, Poppe [7] proposed to plot plate time, t_0/N , against N to obtain a clearer comparison of chromatographic columns. Desmet et al. [8] extended Gidding's concept and generated a broad family of kinetic plots which allow the direct comparison of the performance of different LC supports. Since its introduction, applications of Poppe plots become widespread in development and evaluation of stationary phases and efficient chromatographic methods. Even if Poppe plots were constructed for isocratic separations originally, they were extended for gradient [9] chromatography as well. In these approaches the gradient times are used instead of t_0 to generate the Poppe plots.

In this chapter, possible concepts are presented for the optimization of chromatographic peak capacities. The majority of the results are dedicated to reversed-phase gradient chromatography, or at least separations modes where the linear solvent strength model [10] applies.

The most important algorithms used for the calculation of results of this chapter are presented in Python programming language¹. The reader can use, modify and share it freely without the permission of the author. The main reasons of using Python in optimization of chromatographic separations are the following:

- Python is free and open source, whereas other closed-source commercial products can sometimes be very expensive,
- Python is easy to read and has relatively short learning curve,
- Python integrates well with other languages (e.g. C/C++, Fortran),
- a large number of general-purpose or more specialized libraries exists for Python,
- a huge scientific community is built up around Python. It is easy to find help and information from other scientists.

¹<https://www.python.org/>

Python has impressive libraries applicable in everyday scientific tasks. The codes shared in this chapter based on NumPy² and SciPy³ libraries. These two libraries together cover most of MATLAB's basic functionality and parts of many of the toolkits. Additionally, they have great documentation and an active community. The figures were generated with the Matplotlib⁴ plotting library which is able to produce publication quality figures in a variety of formats and interactive environments.

As of the writing of this chapter (autumn of 2017), Python 3.6, NumPy 1.13, SciPy 1.0, and Matplotlib 2.0 are the actual versions of the language and libraries. The codes shared in this chapter were tested and worked with these versions. Even if Python language and its libraries are evolving gradually, the codes can be used directly or with slight modification at least a decade after publishing this book most probably. Note that Python uses indentation to structure its programs and scripts into blocks. When using the codes presented in Listings 1.1–1.6, please pay careful attention to the leading spaces at the beginning of lines.

The author of this chapter recommends the installation of a Python distribution. In 2017, the two most popular and complete distributions aimed at the need of scientific community are Anaconda Python Distribution⁵ and Enthought Python Distribution⁶. These distributions contains all the necessary tools and libraries required to run the Python codes presented in Listings 1.1–1.6.

A part of the Python codes used during the construction of figures presented in this Chapter were common in each program. In Listing 1.1, imports of the libraries, definitions of functions and constants that are necessary to run all the other codes are presented. The content of Listing 1.1 should be copied before the codes presented in Listings 1.2–1.6.

1.2 Theory

Peak capacity is the measure of the number of peaks that can fit into an elution time window t_1 to t_n with a fixed — usually unity — resolution [2]. There are several approaches for the derivation of peak capacity. Originally, it was defined by Giddings for isocratic chromatography [1] and subsequently extended by Horváth and Lipsky [11] to gradient elution chromatography. Grushka [12] later also derived an equation for computing peak capacity in gradient elution.

Here, we follow Grushka's approach that is general enough to apply for both isocratic and gradient separations as well. According to this approach, peak capacity of a chromatographic separation can be calculated by the solution of an ordinary differential equation.

²<http://www.numpy.org/>

³<https://www.scipy.org/>

⁴<http://matplotlib.org/>

⁵<http://www.anaconda.com/distribution/>

⁶<http://www.enthought.com/product/enthought-python-distribution>

```

import matplotlib.pyplot as plt      #import of Matplotlib library
import numpy as np                  #import of NumPy library
#import functions from SciPy library
from scipy.optimize import brentq, minimize, curve_fit

def trgrad(tg, fi0, dfi, t0, S, k0):
    """
    Calculation of gradient retention time.
    For meaning of parameters, see Eqs. (1.12)-(1.21)
    """
    b = S*dfi/tg*t0
    kfi0 = k0*np.exp(-S*fi0)
    return t0*(1 + np.log(1+kfi0*b)/b)

def peakcap(tg, fi0, dfi, t0, H, L, S, k0):
    """
    Calculation of gradient peak capacity.
    For meaning of parameters, see Eqs. (1.12)-(1.21)
    """
    N = L/H
    b = S*dfi/tg*t0
    kfi0 = k0*np.exp(-S*fi0)
    kL = kfi0/(1+kfi0*b)
    p = b*kfi0/(1+kfi0)
    Theta = np.sqrt((1+p+1/3*p**2))/(1+p)
    Q = np.sqrt(1 + b + 1/3*b**2)
    tau = 1+kfi0*b
    return 1 + np.sqrt(N)/4/Q*np.log((b/6 + 1/b*(Q**2*tau-1) + Theta*Q*tau*(1+kL))/(1+b/2+Q))

def peakcapProduction(tg, fi0, t0, H, L, S, k0):
    """
    Calculation of gradient peak capacity production, (tG+t0)/n.
    For meaning of parameters, see Eqs. (1.12)-(1.21)
    """
    dfi = brentq(lambda dfi: trgrad(tg, fi0, dfi, t0, S, k0)-t0-tg, 1e-6, 1-fi0)
    return (tg+t0)/peakcap(tg, fi0, dfi, t0, H, L, S, k0)

def h(nu, A, B, C):
    """
    Calculation of height equivalent to a theoretical plate.
    For meaning of parameters, see Eqs. (1.31) and (1.32)
    """
    return A*nu**(1/3)+B/nu+C*nu

A, B, C = 1.0, 1.5, 0.05      #parameters of Knox equation Eq (1.31)
fi = 1e3                    #column resistance factor
eta = 1e-3                  #dynamic viscosity (Pa sec),
dm = 1e-9                   #diffusion coefficient, m2/sec

```

Listing 1.1: Libraries, constants, and function definitions necessary to run Listings 1.3–1.6.

$$\frac{dn}{dt} = \frac{1}{w(t)} \quad (1.1)$$

with the following initial condition

$$n(t_1) = 1 \quad (1.2)$$

where w is peak width generally referred as four times standard deviation of a chromatographic peak ($w = 4\sigma$), t is time, and t_1 the retention time of the first eluting compound.

The solution of Eq. (1.1) requires the knowledge of peak widths as a function of retention time, $w(t)$. The general solution can be written as

$$n = 1 + \int_{t_1}^{t_n} \frac{1}{w(t)} dt \quad (1.3)$$

where t_n is the retention time of the last peak. Accordingly, the width of accessible separation window is $t_n - t_1$.

1.2.1 Peak capacity in isocratic elution

Under isocratic elution conditions, the velocity of the sample bands are constant throughout the column. Widths of peaks affected solely by kinetic processes⁷. The dependency of peak widths on retention time can be written as

$$w(t) = \frac{4}{\sqrt{N}} t \quad (1.4)$$

Therefore, solution of Eq. (1.1) is

$$n = 1 + \frac{\sqrt{N}}{4} \ln \frac{t_n}{t_1} \quad (1.5)$$

t_n can be rewritten as the sum of t_1 and the relative retention window

$$t_n = t_1 (1 + \delta) \quad (1.6)$$

where δ is the width of retention window relative to the retention time of the first compound

$$\delta = \frac{t_n - t_1}{t_1} \quad (1.7)$$

Note that δ is the retention factor, k , when t_1 equals to the column hold up time, t_0 .

⁷This statement is strictly true only under linear conditions when the isotherm of compounds are linear. Under non-linear conditions, thermodynamic processes also influence peak shapes.

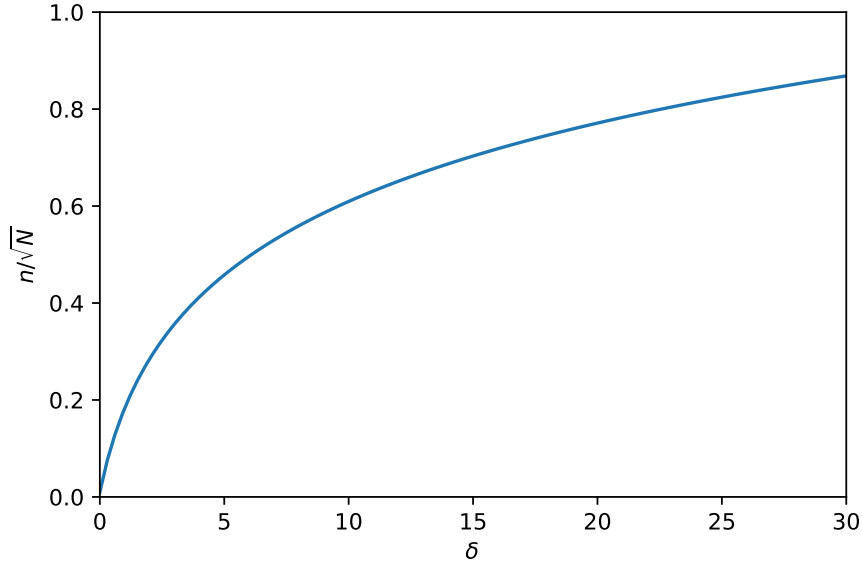


Figure 1.1: Isocratic peak capacity relative to the square root of N as a function of relative retention window, δ .

By combining Eqs. (1.5)–(1.7) peak capacity can be expressed as

$$n = 1 + \frac{\sqrt{N}}{4} \ln(1 + \delta) \quad (1.8)$$

In Fig. 1.1, the isocratic peak capacity relative to the square root of N can be seen as a function of δ . The figure shows that the wider the retention window the higher the achievable peak capacity is. The increase of n , however, is less remarkable at larger δ values.

It is important to note that peak capacity of isocratic separations is not the ratio of the retention window and average peak width. That would be

$$\frac{t_n - t_1}{\bar{w}} = \frac{t_n - t_1}{\frac{1}{t_n - t_1} \int_{t_1}^{t_n} w(t) dt} = \frac{\sqrt{N}}{2} \frac{t_n - t_1}{t_n + t_1} \quad (1.9)$$

In the equations above, the extra column band broadening was not taken into account. In several cases, however, extra column processes have a large impact on the width of peaks. Assuming that the extra column variance is σ_{ext}^2 , peak widths and peak capacities can be rewritten as

$$w(t) = 4\sqrt{\frac{t^2}{N} + \sigma_{\text{ext}}^2} \quad (1.10)$$

and

$$n = 1 + \frac{\sqrt{N}}{4} \ln \frac{1 + \delta + \sqrt{(1 + \delta)^2 + \frac{\sigma_{\text{ext}}^2}{\sigma_1^2}}}{1 + \sqrt{1 + \frac{\sigma_{\text{ext}}^2}{\sigma_1^2}}} \quad (1.11)$$

where σ_1^2 is the variance of the first eluting peak.

1.2.2 Peak capacity in gradient elution

In gradient chromatography, eluent composition is varied during the separation in order to gradually decrease the retention of solutes. Estimation of retention times and peak widths requires the solution of two ordinary differential equations [13] and the knowledge of the change of eluent composition as a function of time, $\varphi(t)$ and the relationship between the retention factor and eluent composition, $k(\varphi)$. In gradient chromatography, it is impossible to derive general equations for the estimation of peak capacity due to the wide variety of the parameters that affect peak shapes. Several assumptions has to be defined regarding the shape of gradient and retention behavior of compounds.

Poppe et al. [13] derived simplified equations for the calculation of retention times and peak variances in the case of linear gradients and linear solvent strength (LSS) behavior that means that the composition of stronger eluent component was a linear function of time, and that the isocratic retention of a solute ($\ln k$) was assumed to be a linear function of the volume fraction of the stronger eluent modifier (φ):

$$k = k_0 \exp(-S\varphi) \quad (1.12)$$

where k_0 the retention factor of the compounds for $\varphi = 0$, $-S$ the slope of $\ln k[\varphi]$ vs. φ plot. S is a practical measure of the retention sensitivity of a compound toward the change of eluent composition.

Under these conditions, the retention time of a compound, t_R , and the width of its peak can be calculated by the following set of equations [13]:

$$t_R = t_0 \left(1 + \frac{\ln(k_{\varphi_0} b + 1)}{b} \right) \quad (1.13)$$

$$w = 4 \frac{L}{\sqrt{N}} \frac{1 + k_L}{u_0} \Theta \quad (1.14)$$

with b the gradient steepness

$$b = S t_0 \frac{\Delta\varphi}{t_G} \quad (1.15)$$

where $\Delta\varphi$ is the change of stronger eluent component in t_G gradient time, k_L the retention factor of the compound at the column outlet. Θ represents the band compression [14, 15] that arises from the rear part of the band migrating at a velocity higher than the front part.

$$k_L = \frac{k_{\varphi_0}}{1 + k_{\varphi_0} b} \quad (1.16)$$

and

$$\Theta = \frac{\sqrt{1 + p + \frac{1}{3}p^2}}{1 + p} \quad (1.17)$$

where

$$p = b \frac{k_{\varphi_0}}{1 + k_{\varphi_0}} \quad (1.18)$$

and k_{φ_0} is the retention factor of solute at the beginning of analysis ($\varphi = \varphi_0$)

By rearranging Eq. (1.13) for k_{φ_0} and substituting it into Eq. (1.14), $w(t)$ can be generated. It still cannot be integrated since the value of b is different from solute to solute. Accordingly, an additional assumption has to be made regarding the constant values of S for all the sample compounds. In that case, peak capacity of linear gradients in case of LSS behavior becomes

$$n = 1 + \frac{\sqrt{N}}{4} \frac{1}{Q} \ln \left(\frac{\frac{b}{6} + \frac{1}{b} (Q^2 \tau_n - 1) + \Theta_n Q \tau_n (1 + k_{L,n})}{1 + \frac{b}{2} + Q} \right) \quad (1.19)$$

with

$$Q = \sqrt{1 + b + \frac{1}{3}b^2} \quad (1.20)$$

and

$$\tau_n = \exp \left[b \left(\frac{t_n}{t_0} - 1 \right) \right] \quad (1.21)$$

where $k_{L,n}$ and Θ_n refers to the last eluting compounds [see Eqs. (1.16) and (1.17)]. Note that Eqs. (1.19)–(1.21) are essentially the same as Eqs. (14)–(17) of Ref. [16] derived by Gritti and Guiochon. However, here they are presented in a different grouping of parameters.

In Fig. 1.2, gradient peak capacities as a function of t_G can be seen at different combination of S and k_0 parameters. As opposed to isocratic separations (see Fig 1.1), peak capacities approach a maximal peak capacity as analysis time increases in gradient separations. The maximal peak capacity that can be achieved with gradient elution can be determined as the limit of Eq. (1.19) as t_G approaches infinity.

$$n_{\max} = 1 + \frac{\sqrt{N}}{4} \ln(1 + k_{\varphi_0,n}) \quad (1.22)$$

where $k_{\varphi_0,n}$ is the retention factor of the last eluting compound at the beginning of analysis.

Peak widths and peak capacities calculated by Eqs. (1.14) and (1.19) are valid in ideal case.

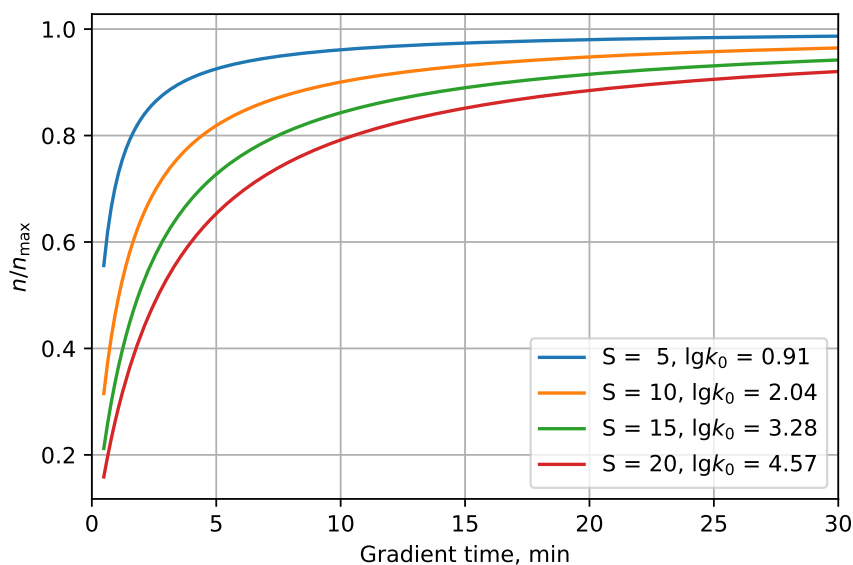


Figure 1.2: Gradient peak capacity relative to n_{\max} as a function of gradient time, t_G . Parameters of calculation: column length $L=10$ cm, particle diameter $d_p=1.7$ μm , pressure drop $\Delta P=1200$ bar, plate count $N=25\,000$, column hold-up time $t_0=28.8$ sec.

In practice, several effects cause peak broadening downstream the column (e.g., peak spreading in tubings, connections, detector cell, etc.). Since the retention factors of compounds are large at the beginning of analysis, solutes are focused in narrow bands at the head of column after injection. Therefore, the pre-column effects usually do not affect final peak shapes. Thus, the peak variance has to be completed with the contributions of post column broadening. Accordingly, widths of detected peaks can be calculated as:

$$w \simeq 4 \sqrt{\frac{L^2}{N} \left(\frac{1+k_L}{u_0} \right)^2 \Theta^2 + \sigma_{t,\text{pc}}^2} \quad (1.23)$$

where $\sigma_{t,\text{pc}}^2$ represents the contribution of the post-column processes to the variance of the peak.

1.3 Optimization of peak capacity

In practice, optimization of peak capacities are necessary when the sample contains large number of compounds. In that case the goal usually is not the complete baseline separation of all compounds, but the spreading of analytes as much as possible before introduction into mass spectrometer or a second chromatographic dimension. The analyst usually has two different goals: (1) achieving a given target peak capacity within as short time as possible, or (2) reaching the highest possible peak capacity in a given analysis time. In the following general con-

cepts and considerations are presented that are applicable to fulfill both goals of peak capacity optimization.

1.3.1 Optimization of isocratic separations

Close examination of Eq. (1.11) highlights that peak capacity in isocratic mode can be optimized by:

- minimizing the extra-column band broadening (σ_{ext}^2),
- maximizing the retention window (δ), and
- maximizing column efficiency (N).

Extra-column band broadening

It is well known that extra column band broadening has a deteriorating effect on separation performance. The relative decrease of apparent column plate count depends on the relation of column- and extra-column variances.

$$\frac{\Delta N}{N} = -\frac{\sigma_{\text{ext}}^2}{\sigma_{\text{col}}^2 + \sigma_{\text{ext}}^2} = -\frac{\sigma_{\text{ext}}^2}{\frac{t_R^2}{N} + \sigma_{\text{ext}}^2} \quad (1.24)$$

Typical values of contributions of UHPLC, optimized HPLC, and non-optimized HPLC systems to the peak variances are 5, 25, and 100 μL^2 [17, 18], respectively⁸. Note, however, that the actual values vary from instrument to instrument. Since column variance is proportional to the square of retention time, the deteriorating effect of extra-column band broadening is more significant for the early eluting compounds. In Fig. 1.3, the decrease of peak capacities can be seen as $\sigma_{\text{ext}}^2/\sigma_1^2$ ratio varies. The volumetric variance of a peak eluted at the hold-up time from a 150×4.6 mm column packed with 5 μm particles is typically larger than 175 μL^2 . Therefore, $\sigma_{\text{ext}}^2/\sigma_1^2$ is lower than 0.5 when an older HPLC instrument is used. Less than 5% decrease of peak capacity should be expected in that case. Using a 50×2.1 mm column packed with 1.7 μm particles, however, the variance of the peak eluting with the column dead volume can be less than 1 μL^2 . Even a state of the art instrument with a 5 μL^2 extra column variance can decrease the peak capacity with more than 10%. Using these columns in outdated, non-optimized instrument, the peak capacity might be lower than half of that provided by the column itself. The effect of σ_{ext}^2 is more significant when the retention window is narrow. Note, that

⁸Because of practical reasons, volumetric variances are usually used for the quantification of extra column band broadening (see Refs. [17, 18]). By dividing it with the square of flow rate, volumetric variances can be converted to temporal variances. Similarly, temporal variances can be converted to volumetric ones by multiplying with the square of flow rate. Therefore, volumetric variance of a chromatographic peak is the ratio of square of retention volume to the plate number, V_R^2/N .

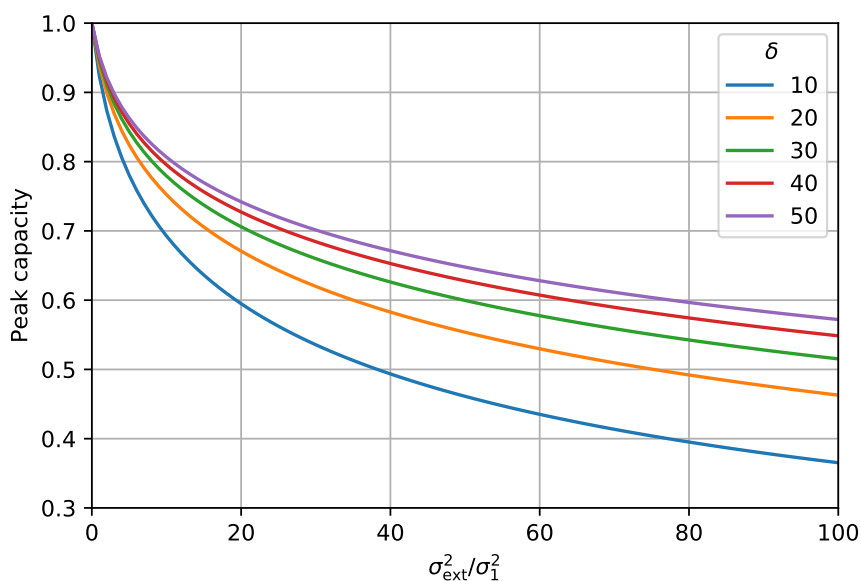


Figure 1.3: Relative peak capacity as a function of ratio of extra-column and column variance at different width of retention window δ .

the decrease of peak capacity is unaffected by the actual column plate number in practice when N is sufficiently large.

It can be concluded that extra-column processes might have significant effect on the achievable peak capacity depending on the type of column and instrument used. Accordingly, the extra column effects cannot be neglected in the optimization of isocratic peak capacities, especially when ultra-high performance columns are used. The minimization of σ_{ext}^2 by reducing volumes of capillaries and detector is necessary when the goal of separation is to achieve high peak capacities in a reasonable analysis time.

Width of retention window

Eq. (1.11) clearly shows that the wider the retention window the more powerful the separation is. After some simple considerations, the relative retention window, δ , can be rewritten as

$$\delta = \begin{cases} (\alpha - 1) \frac{k_1}{1+k_1} & \text{if } k_1 > 0 \\ k_n & \text{if } k_1 = 0 \end{cases} \quad (1.25)$$

where α is the selectivity of the last and first eluting solutes, $\alpha = k_n/k_1$.

Eq. (1.25) has similar form than the simplified resolution equation that is one of the most important relationships in development and optimization of isocratic separations (see e.g. Eq. (2.24) of Ref. [19]). Eq. (1.25) serves with the important conclusion that peak capacity

of isocratic separations can be improved by the increase of α .

The selectivity between the first and last eluting solutes can be adjusted by the proper choice of stationary phase and separation conditions. Variation of mobile phase composition can be a suitable strategy if the compounds respond differently to the change of eluent composition. In reversed phase and hydrophilic interaction modes this condition applies usually. Especially in the case of analysis of biological samples. In ion chromatography, however, only selectivities of ions having different charge can be modified by the change of the concentration of electrolyte. When the ions have the same charge, other approaches should be applied for the variation of α (e.g. addition of organic modifier to the eluent).

The change of separation temperature can also be a suitable option for the selectivity improvement. Especially, when the difference between the adsorption enthalpies, ΔH , of the first and last eluting compounds are large. Since late eluting solutes usually have higher affinities toward the stationary phase, the decrease of temperature might improve α . Note, however, that it increases the pressure drop of the column and might decrease the overall column efficiency significantly.

Eq. (1.25) shows that by increasing the retention factor of the first eluting peak, k_1 , peak capacity of isocratic separation can also be improved supposing that α remains constant. Note, however, that this scenario is rather theoretical, it does not have any significance in practice. Increasing the retention of the first eluting compound while α is kept constant would increase the analysis time so drastically that the cost of analysis in time and solvent consumption would be too much for the extra information gained by the improved peak capacity. Instead, during the optimization of isocratic separations, α should be maximized by increasing k_n and decreasing k_1 as low as possible, ideally until zero.

It is worth studying the rate of peak capacity production, v_n , with the increase of analysis time. Rate of peak capacity production can be defined as

$$v_n = \frac{dn}{dt_n} = \frac{1}{4} \frac{\sqrt{N}}{t_n} \quad (1.26)$$

Eq. (1.26) reveals that v_n is the highest at the beginning of chromatogram ($t_n = t_0$) and it decreases gradually as the time passes. The rate of peak capacity production relative to the initial v_n is given by

$$v_{n,rel} = \frac{\frac{1}{4} \frac{\sqrt{N}}{t_n}}{\frac{1}{4} \frac{\sqrt{N}}{t_0}} = \frac{1}{1 + k_n} \quad (1.27)$$

In Fig. 1.4, $v_{n,rel}$ can be seen as a function of retention factor of the last eluting component. It is obvious that the most peak capacities gained close to the hold up time of the column. As the analysis time increases, the rate of peak capacity production decreases remarkably. This

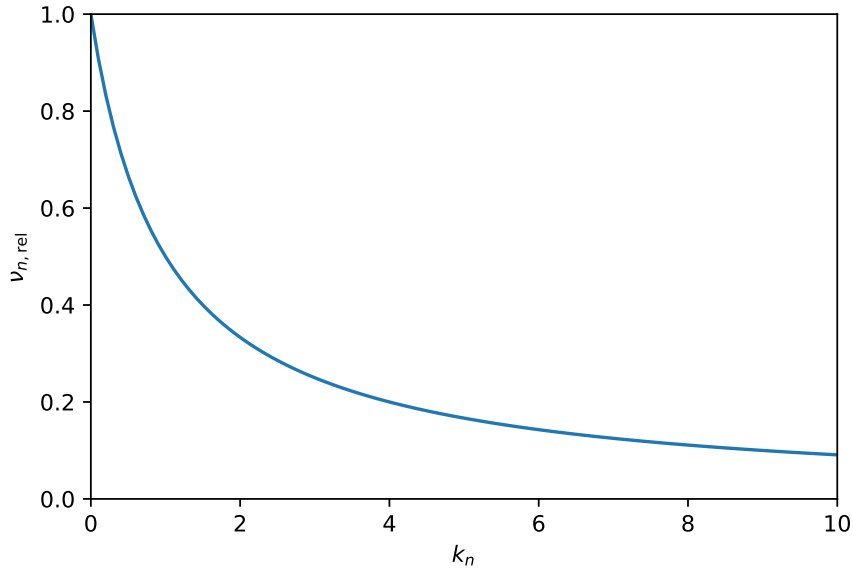


Figure 1.4: Rate of peak capacity production relative to the initial v_n .

is due to the fact that peaks become wider as their retention time increase as it is shown by Eq. (1.4). As the retention of compounds increases their migration velocity decreases and more and more time is necessary to elute one band from the chromatographic column.

A 20-peak-capacity chromatogram can be seen in Fig. 1.5. The figure clearly shows the peak generation phenomenon discussed above. Most of the eluted peaks appear at the beginning of the chromatogram. Late eluting peaks are wider and more time is necessary to ensure unity resolution between them. Half of the total peak capacities generated in the first third of the analysis time. Figs. 1.4 and 1.5 emphasize the importance of reducing the retention of the first eluting peak. These figures also highlights the necessity of reducing extra column broadening since most of the peak capacities are generated in the beginning of analysis time. The narrow, early eluting peaks are more sensitive toward the detrimental effect of extra column processes.

Specific peak capacity production, n' , shows how much total peak capacities generated in a given unit of time. It can be defined as

$$n' = \frac{n}{t_n} \quad (1.28)$$

Specific peak capacity production has an optimum at

$$t_{n,opt} = t_1 \exp\left(1 - \frac{4}{\sqrt{N}}\right) \simeq 2.718 t_1 \quad (1.29)$$

with a maximal value of

$$n'_{opt} = \frac{1}{t_{n,opt}} \frac{\sqrt{N}}{4} \simeq 0.092 \frac{\sqrt{N}}{t_1} \quad (1.30)$$

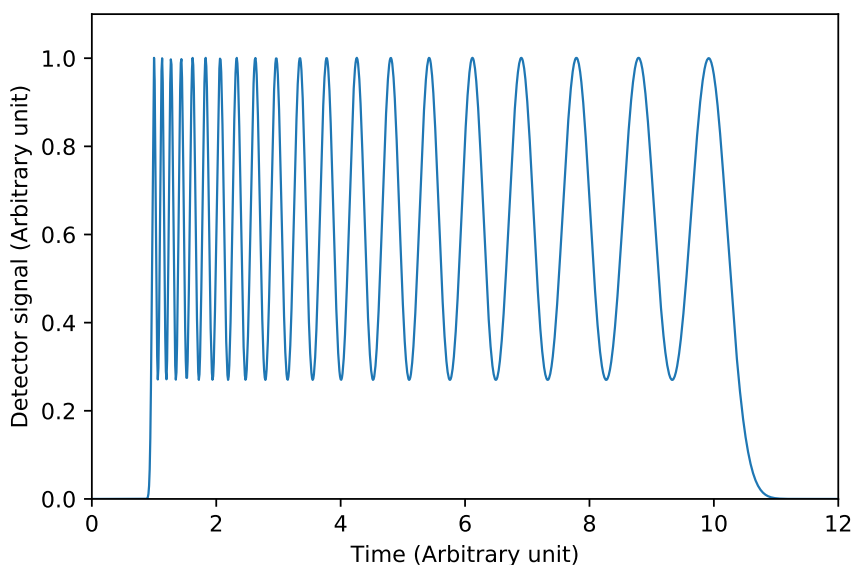


Figure 1.5: Chromatogram of a 20-peak-capacity separation in case of isocratic elution.

In Fig. 1.6, specific peak capacity production can be seen as a function of analysis time. Note that the time axis is scaled for $t_{n,\text{opt}}$ and the y axis is scaled for n'_{opt} . The figure clearly represent that the specific gain of peak capacity decreases by the increase of analysis time. Accordingly, the analyst has to make a trade off between the the analysis time and separation power of the chromatographic system in the knowledge of the sample composition analyzed.

Plate number

A third option for the increase of peak capacity is the optimization of number of theoretical plates, N . In order to estimate column efficiency under different separation conditions, one should choose a proper plate height or plate number model. The most accurate equation for describing the dependence of the plate height on mobile phase linear velocity is offered by the general rate model. It is, however, so complex that it is rarely used in method development. The van Deemter and the Knox equations are the most widely used plate height equations in practice. The simple form of the analytical solution for the minimum plate height obtained from van Deemter's equation allows one to locate the optimum velocity and minimum plate height and to obtain insight into the contribution of kinetic processes to it. The Knox equation, however, provides better fit to liquid chromatography data than van Deemter equation. Therefore it will be used in the following.

Knox equation can be defined as

$$h = A v^{\frac{1}{3}} + \frac{B}{v} + C v \quad (1.31)$$

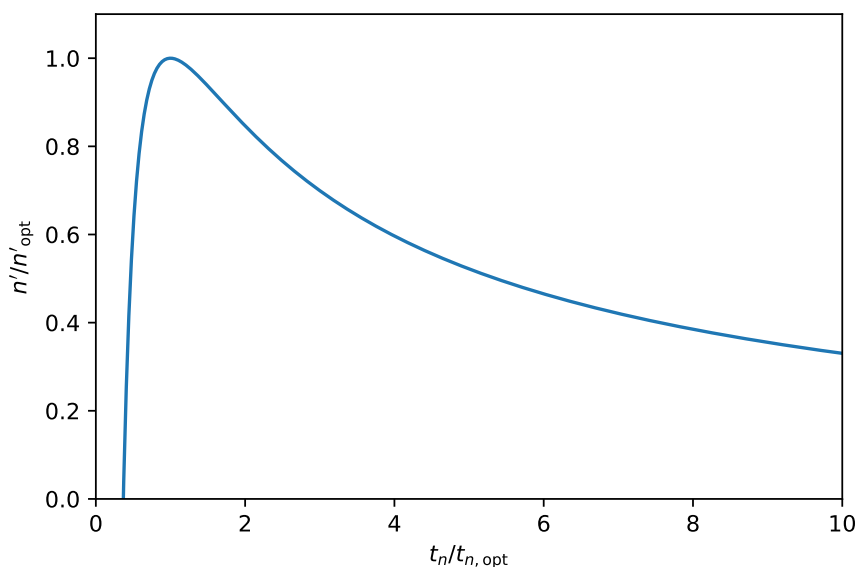


Figure 1.6: Specific peak capacity production, Eq. (1.30), as a function of analysis time.

where A , B , and C are dimensionless constant parameters. Their typical values are 0.8–1.0, 1.5, and 0.02–0.05, respectively, h the reduced plate height that is the ratio of the height equivalent to a theoretical plate and the particle diameter, $h = H/d_p$, and v the reduced velocity.

$$v = \frac{u_0 d_p}{D_m} \quad (1.32)$$

where u_0 is the linear velocity of the mobile phase, d_p the particle size and D_m the diffusion coefficient of the solute molecules. Note that the reduced velocity is the same as the Péclet number used in study of transport phenomena.

An obvious way of peak capacity optimization in isocratic chromatography is the minimization of Eq. (1.31). Unfortunately, the exact solution of the minimum plate height based on Knox equation is too complicated to be informative. In Listing 1.2, however, a simple Python code is presented for obtaining the parameters of Knox plate height equation, and the optimal eluent velocity.

As it was discussed in the introduction, a popular approach of characterization and comparison of column performances is the use of Poppe plots. In a single graph, it includes information on the plate number, the analysis time, and the maximum pressure that can be applied with the chromatographic system. Therefore, it is more capable for optimization purposes than a single plate height equation. In a Poppe plot, the plate time (H/u_0 or N/t_0) is plotted against separation efficiency. During the construction of these plots it is assumed that the chromatographic system is operated at the maximum allowed pressure, ΔP . The latter can be described by the

```

#-#-#-#   Use with Listing 1.1   #-#-#-#

#Experimental data. Replace with actual data!
#eluent linear velocities, m/s
u0s = np.array([9.62e-05, 1.443e-04, 1.924e-04, 2.405e-04, 3.849e-04,\
                4.811e-04, 9.623e-04, 1.4435e-03, 1.9247e-03, 2.4059e-03,\
                2.8871e-03, 3.3683e-03, 3.8495e-03, 4.3307e-03, 4.8119e-03,\
                5.2931e-03, 5.7743e-03, 6.2555e-03, 6.7367e-03, 7.2179e-03,\
                7.6991e-03, 8.1802e-03])
#number of theoretical plates at u0s eluent velocities
Ns = np.array([3377.5, 4773.7, 6232.9, 7110.8, 9453.8, 11123.4,\
              14019.4, 14868.8, 14336.9, 13828.5, 13666.4, 12903.1, 12553.7,\
              12279.4, 11725.8, 11183.2, 11100.6, 10710.1, 10196.1, 10023.4,\
              9899.3, 9699.0])

dp = 1.7e-6           #particle diameter, m
L = 0.05             #column length, m
nus = u0s*dp/dm      #eluent reduced velocities
Hs = L/Ns            #heights equivalent to a theoretical plate, m

fp, fcv = curve_fit(h, u0s*dp/dm, Hs/dp) #fitting Knox equation on experimental data
A, B, C = fp[0], fp[1], fp[2]           #parameters of Knox equation
print('A = {0:.3f}, B = {1:.3f}, C = {2:.3f}'.format(A, B, C)) #print results

opt = minimize(h, 2, args=(A, B, C))    #minimize Knox equation with parameters A, B, C
print('Minimum reduced HETP: {0:.3f}, minimum HETP: {1:.3f} um'\
      .format(opt.fun, opt.fun*dp*1e6))  #print minimum HETP
print('Optimal reduced velocity: {0:.3f}, optimal velocity: {1:.3f} cm/min'\
      .format(opt.x[0], opt.x[0]*dm/dp*100*60)) #print optimal velocity

```

Listing 1.2: Python code for determination of parameters of Knox plate equation.

Kozeny-Carman equation

$$\Delta P = \frac{\phi u_0 \eta L}{d_p^2} \quad (1.33)$$

where L is the column length, η the dynamic viscosity of the eluent, and ϕ the column resistance factor which is in the range of 500–1000 (1000 is assumed in this work).

Considering that the column length, L , is the product of the required plate count, N_{req} , and the plate height (that is $h d_p$), Eq. (1.33) can be rewritten as

$$\Delta P = \frac{\phi u_0 \eta N_{\text{req}} h}{d_p} \quad (1.34)$$

From Eq. (1.34) it is possible to calculate the maximal plate number generated when the column work at the optimal eluent velocity.

$$N_{\text{opt}} = \frac{d_p^2 \Delta P}{v_{\text{min}} D_m \eta \phi h_{\text{min}}} \quad (1.35)$$

where h_{min} is the minimum reduced plate height obtained at v_{min} optimal reduced eluent velocity.

The column length necessary to generate N_{opt} plate numbers is

$$L_{\text{opt}} = N_{\text{opt}} h_{\text{min}} d_p = \frac{d_p^3 \Delta P}{v_{\text{min}} D_m \eta \phi} \quad (1.36)$$

with a dead time of

$$t_{0,\text{opt}} = \frac{N_{\text{opt}}^2 h_{\text{min}}^2 \eta \phi}{\Delta P} = \frac{d_p^4 \Delta P}{v_{\text{min}}^2 D_m^2 \eta \phi} \quad (1.37)$$

Note that Eq. (1.35) is not the maximum plate number that can be generated by the given stationary phase. N_{opt} is the maximum achievable plate count when the column is operated at the optimal eluent velocity and the column length is maximized in order to reach ΔP . The overall maximum of plate number is

$$N_{\text{max}} = \frac{d_p^2 \Delta P}{B D_m \eta \phi} \quad (1.38)$$

where B is a parameter of the plate height equation Eq. (1.31). If van Demter equation is used to estimate column efficiency, N_{max} becomes the same mathematically as in case of Knox equation. Considering the typical values of B , v_{min} and h_{min} , it can be predicted that N_{max} is ~ 3 -times larger than N_{opt} . This observation serves with the important conclusion that plate number can be further increased by using longer columns even if the eluent velocity becomes smaller than the optimal one.

The minimum reduced plate height of a well packed column is ~ 2.0 in case of fully porous, and ~ 1.7 in case of core-shell phases with optimal reduced flow rate 2.0–3.0. Assuming that v_{\min} is 2.8, N_{opt} of a column packed with $1.7 \mu\text{m}$ fully porous particles operated at 1200 bar pressure is 62 000 for small molecules ($D_m = 10^{-9} \text{ cm}^2/\text{sec}$). A 21 cm long column with a slightly more than 2 min dead time is necessary to obtain this separation performance. For $5 \mu\text{m}$ particles and 400 bar pressure drop, N_{opt} is larger, $\sim 180\,000$. This efficiency can be generated with a 1.8 m long column and 53 min dead time.

Eqs. (1.35)–(1.38) serve with important conclusions. The achievable plate number is directly proportional to the applied pressure and to the square of particle diameter. Accordingly, the larger particles used, the higher plate number can be generated by the chromatographic system. A two-fold increase of d_p can produce four-times more plates. It was shown in Eq. (1.8) that the peak capacity is proportional to the square root of N . Therefore, n is directly proportional to the particle diameter and to the square root of pressure of separation. One can generate more peak capacities by using larger particles and higher operating pressures. In the same time, however, the time of analysis increase with the fourth power of d_p . It means that a two-fold increase of peak capacity requires 16-times more analysis time and an 8-times more longer column if the peak capacity is increased by the duplication of particle size. The same improvement can be achieved by the quadruplication of the pressure. In that case both the analysis time and column length are quadrupled. Note that these conclusions are valid numerically only for columns operated at the optimal eluent velocity. The tendencies, however, are valid in any eluent conditions.

In Eq. (1.35) there is no column length. The idea behind Eq. (1.35) is that the column work at the optimal flow rate that produces the minimal plate height. The column length is adjusted in order to generate the maximal pressure drop, ΔP . In the construction of Poppe plots, the same approach can be used with the difference that the eluent velocity is varied in order to generate the required plate number. The following equation is solved for v

$$\frac{\Delta P d_p}{\phi \eta N_{\text{req}}} - \frac{v D_m}{d_p} h = 0 \quad (1.39)$$

Note that h is a function of v .

The plate height, plate number, column length and dead time are calculated by the appropriate substitutions into Eqs. (1.31) and (1.35)–(1.37). By plotting H/u_0 or N/t_0 against N_{req} , the Poppe plot can be constructed.

A simplified approach for the construction of Poppe plot is to vary column length in a wide range. It defines the value of u_0 from Eq. (1.33). u_0 allows the calculation of plate height by Eq (1.31), then the plate number as L/H , and the dead time as L/u_0 . By plotting N/t_0 against N_{req} , the Poppe plot can be constructed. In Listing 1.3, this simplified approach is presented for

```

##-##-## Use with Listing 1.1 ##-##-##

ls = np.logspace(-4, 2, 1000)      #definition of range of column lengths

#-----CONSTRUCTION OF POPPE PLOTS-----#
#iterate through  $d_p$  -  $\Delta P$  data pairs,
#dp - particle diameter, dP - max pressure drop
for dp, dP in [(1.3e-6, 1200e5), (1.7e-6, 1200e5), (1.7e-6, 400e5), (3e-6, 600e5), \
              (5e-6, 400e5)]:
    u0s = dP*dp**2/(fi*eta*ls)      #eluent linear velocities, see Eq. (1.33)
    nus = u0s*dp/dm                 #reduced velocities, Eq. (1.32)
    Ns = ls/(h(nus, A, B, C)*dp)    #number of theoretical plates
    t0s = ls/u0s                    #dead times
    plt.loglog(np.sqrt(Ns), t0s/np.sqrt(Ns)) #plot results

#-----PLOTTING OF CONSTANT  $t_0$  LINES-----#
Ns = np.logspace(2,6,10)           #definition of range of plate numbers
#iterate through different  $t_0$ s
for t0 in [1e-1, 1e0, 1e1, 1e2, 1e3, 1e4]:
    #at each  $t_0$ , plot  $t_0/\sqrt{N}$  with black dashed line
    plt.loglog(np.sqrt(Ns), t0/np.sqrt(Ns), 'k--', linewidth=0.5)

plt.xlim(1e1,1e3)                  #set x limits
plt.ylim(1e-3,1e2)                 #set y limits
plt.xlabel(r'$\lg \sqrt{N}$')       #set label of x axis
plt.ylabel(r'$\lg t_0 / \sqrt{N}$') #set label of x axis
plt.show()                          #show plot

```

Listing 1.3: Python code for construction of Poppe plot.

the construction of Poppe plot. It can be seen that this approach does not need any numerical optimization algorithm.

In Fig. 1.7, Poppe plot of different diameter column packings can be seen. The pressure drop is varied according to the typical maximum pressure used with these particles. Since square root of N is required for the estimation of isocratic peak capacities, t_0/\sqrt{N} is plotted against \sqrt{N} in the figure. Since the value of $\frac{\ln(1+\delta)}{4}$ in Eq. (1.8) is close to unity under most of the practically relevant conditions ($\delta > 15$), Fig. 1.7 can be considered as a kinetic plot of isocratic peak capacities. The diagonal lines represent zones of constant analysis times.

Fig. 1.7 demonstrates clearly that, in the practically relevant range of analysis times ($t_0 = 10 - 100$ sec), higher peak capacities can be generated with columns packed by smaller packing material than by larger ones provided that each column is operated at the highest allowed pressures. Similarly, it is possible to achieve the same peak capacity in significantly shorter analysis times by applying ultra-high performance stationary phases. The advantages of larger particle sizes arose when the goal is to produce very high peak capacities (>500). The vertical asymptotes correspond to the square root of maximal plate counts as it is calculated by Eq. (1.38). As it can be seen, with the use of larger particles higher peak capacities can be achieved. The cost of this separation power is the extremely large analysis time, however. The figure also emphasize that the use of $1.7 \mu\text{m}$ particles in a 400-bar HPLC system does not offer

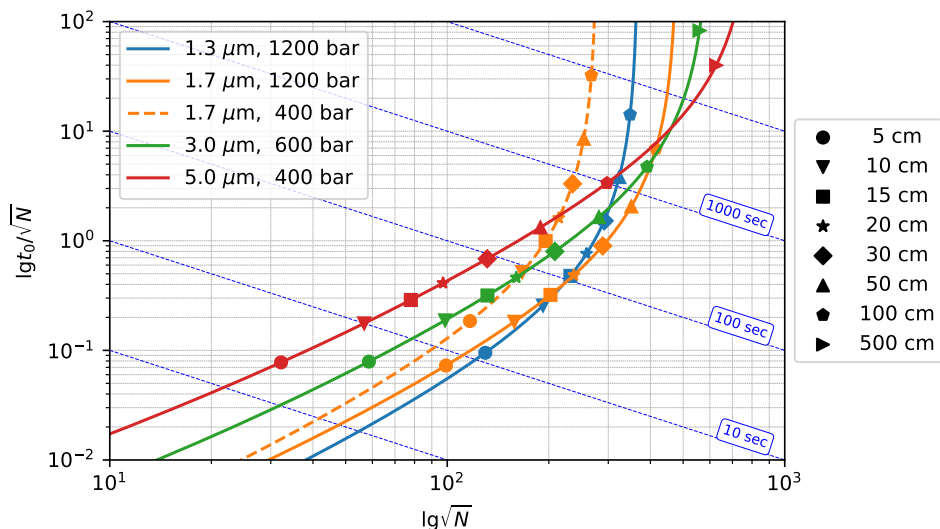


Figure 1.7: Poppe plot of isocratic peak capacity. Parameters of calculations: maximal pressure drop $\Delta P=400$ bar, viscosity $\eta=0.001$ Pa s, flow resistance factor $\phi=1000$, diffusion coefficient $D_m=10^{-9}$ m/s, reduced plate height expression Eq. (1.31) with parameters $A=1.0$, $B=1.5$, $C=0.05$ [7].

significant improvement over larger particles in the practically relevant range of analysis times.

In general, it can be concluded that when time is not a limiting factor, the peak capacity of an isocratic separation can be maximized by the increase of retention window and the use of large particles and the longest possible columns consistent with the pressure limit of the instrument.

Even if Poppe plot allows detailed comparison of different stationary phases and separation strategies, most of the points on the curves do not have any practical relevance. No one has, e.g., a 17.9 cm long column packed with $5 \mu\text{m}$ particles to generate 8 000 plates. Instead, there are one or more 5, 10, and 15-cm long columns in the drawer. In Fig. 1.7, points calculated for column lengths that are possible to combine from commercially available columns are also presented. These points present the practically relevant separation conditions. By use of these points one can easily compare different separation strategies and decide the most appropriate one considering the required peak capacity and the available instrumentation and consumables present in the analytical lab.

A more complete design and optimization of isocratic separation can be achieved by constructing nomogram-like Poppe plots, as it is shown in Fig. 1.8. This figure is calculated for $1.7 \mu\text{m}$ particles. Red dashed lines represents pressure drops, blue dashed lines the column hold-up times, and thick color lines some typical column lengths that can be combined by connecting commercially available columns. Fig. 1.8 gives a deep insight into the influence of chromatographic conditions on the achievable separation power. It can be concluded that by increasing the column length the plate number can be improved even if ΔP remains constant.

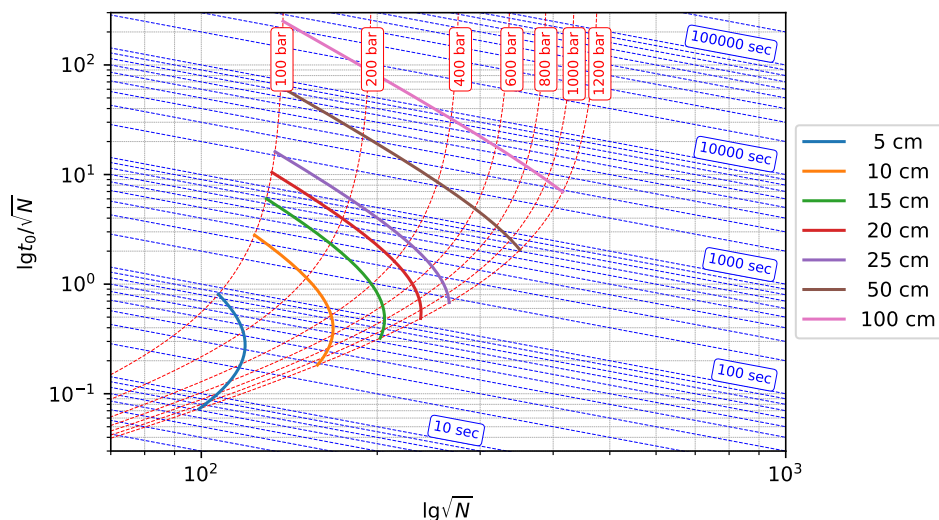


Figure 1.8: Nomogram for the design and optimization of isocratic separation with $1.7 \mu\text{m}$ particles. Parameters of calculation can be found in caption of Fig. 1.7.

The increase of ΔP always decrease the plate time, even if N might decrease since the eluent velocity exceed the optimal one. When the columns are short, it is advantageous to operate the column at the optimal flow rate. At large columns, maximal ΔP is smaller than that would be necessary to produce that eluent flow rate.

Nomograms such as Fig. 1.8 can be used in method development directly. First, the analyst should define the maximal pressure drop applicable. Then, moving along the “isobar”, the column length that produce the desired plate count in an acceptable analysis time can be found. One can generate nomograms like Fig. 1.8 for any phases available in the lab. The optimal column dimensions, stationary phases and operating conditions can be selected directly by the comparison of these nomograms.

In Listing 1.4, a Python code is presented for the generation of nomogram-like Poppe plots. Note that the import of NumPy and Matplotlib packages, the definition of reduced plate height equation and some constant parameters are not included in Listing 1.4. Those can be found in Listing 1.1. Therefore the two codes should be used together in order to generate the nomogram.

1.3.2 Optimization of gradient separations

Extra column broadening

It was shown previously, that extra column band broadening has a detrimental effect on achievable peak capacities in isocratic elution. In Fig. 1.9, a typical 20-peak-capacity chromatogram of gradient separation is shown. The timescale is the same as in Fig. 1.5. It can be seen, that the

```

    ##-##-## Use with Listing 1.1 ##-##-##

dp = 1.7e-6          #definition of particle diameter, m

#-----CONSTRUCTION OF "ISOBARS"-----#
ls = np.logspace(-4,2, 1000)      #definition of range of column lengths
#iterate through different pressure drops
for dP in [100e5, 200e5, 400e5, 600e5, 800e5, 1000e5, 1200e5]:
    u0s = dP*dp**2/(fi*eta*ls)      #eluent velocity, m/sec, see Eq. (1.33)
    Ns = ls/(h(u0s*dp/dm, A, B, C)*dp) #plate numbers
    t0s = ls/u0s                    #column hold up times, sec
    plt.loglog(np.sqrt(Ns), t0s/np.sqrt(Ns), 'r--', linewidth=0.5) #plot isobars

#-----PLOTING OF CONSTANT t0 LINES-----#
Ns = np.logspace(2,6,1000)        #definition of range of plate numbers
#iterate through different t0s
for i in [1e-1, 1e0, 1e1, 1e2, 1e3, 1e4, 1e5]:
    #at each t0, plot t0/sqrt(N) with blue dashed line
    plt.loglog(np.sqrt(Ns), i/np.sqrt(Ns), 'b--', linewidth=0.5)

#-----CONSTRUCTION OF POPPE CURVES FOR DIFFERENT COLUMN LENGTHS-----#
dP = np.logspace(7,np.log10(1200e5), 1000) #definition of pressure range, Pa
#iterate through different column lengths that has practical relevance
for length in [0.05, 0.1, 0.15, 0.2, 0.25, 0.5, 1]:
    u0s = dP*dp**2/(fi*eta*length) #eluent velocity, m/sec, see Eq. (1.33)
    Ns = length/(h(u0s*dp/dm, A, B, C)*dp) #plate numbers
    t0s = length/u0s                #column hold up times, sec
    plt.loglog(np.sqrt(Ns), t0s/np.sqrt(Ns)) #plot Poppe curves in log-log scale

plt.xlim(70,1e3)                  #set x limits
plt.ylim(1e-2,1e3)                #set y limits
plt.xlabel('$\lg \sqrt{N}$')       #label of x axis
plt.ylabel(r'$\lg t_0 / \sqrt{N}$') #label of y axis
plt.show()                         #show plot

```

Listing 1.4: Python code for construction of nomogram-like isocratic Poppe plot.

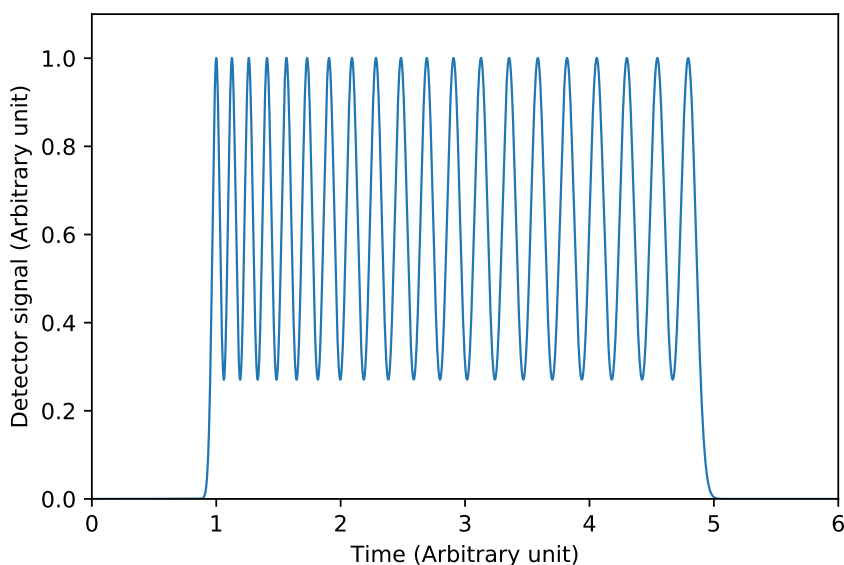


Figure 1.9: Chromatogram of a 20-peak-capacity separation in case of gradient elution.

same peak capacity could be generated in much less time. The peaks in Fig. 1.9 remain narrow throughout the whole separation range. Accordingly, in gradient elution the extra column effects should be more significant than in isocratic runs.

In Fig. 1.10, the relative decrease of peak capacities are shown for a 50×2.1 mm column packed with $1.7 \mu\text{m}$ particles and a 150×4.6 mm column packed with $5 \mu\text{m}$ particles as a function of volumetric extra column variance. Note, that typical values of extra column variances of UHPLC, optimized HPLC, and non-optimized HPLC systems are 5 , 25 , and $100 \mu\text{L}^2$ [17, 18], respectively. Fig. 1.10 emphasize the necessity of minimizing extra column volumes of chromatographic system. Even a state of the art chromatograph can decrease the peak capacity of an ultra-high performance column by 10%. The use of these columns in an obsolete hardware is senseless practically. Even a system with $20 \mu\text{L}^2$ extra column variance – that corresponds to a well optimized conventional HPLC or even some UHPLC systems – might decrease n by 20–40%. For large columns, with large dead volumes, the effect of system volume is less detrimental.

Gradient conditions

Optimization of conditions of gradient separations is a much more complex task than that of isocratic separations. Some of the parameters affecting peak capacity of gradient runs are not mutually independent. Therefore, numerical algorithms should be used in order to find the optimal separation conditions.

Since Poppe plot can be applied directly in isocratic method development (see Fig. 1.8),

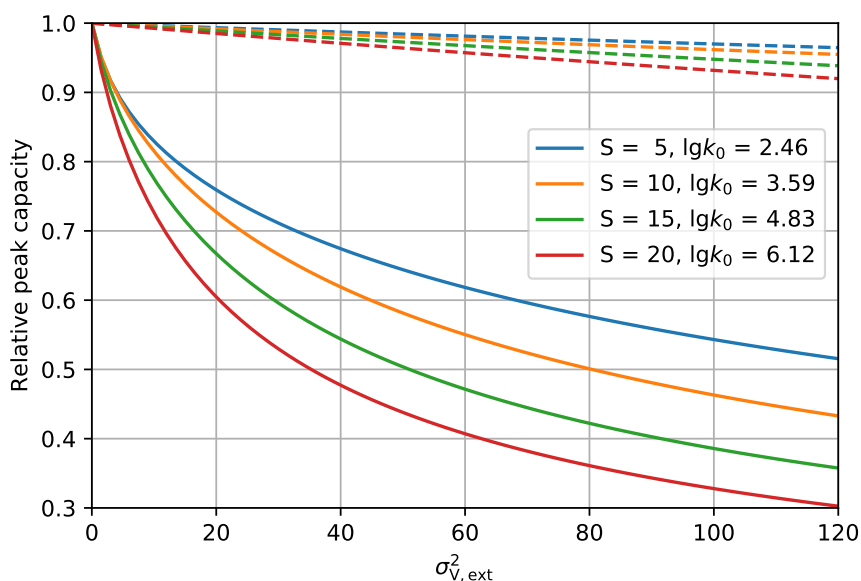


Figure 1.10: Relative decrease of gradient peak capacity as a function of extra column variance. Solid lines: 50×2.1 mm column packed with $1.7 \mu\text{m}$ particles ($H = 2.81$), dashed lines: 150×4.6 mm column packed with $5 \mu\text{m}$ particles ($H = 2.97$).

it would be useful to apply the same concept in gradient runs as well. There are several approaches to construct gradient kinetic plots [9, 20–24]. Here, we use Eq. (1.19) as the basis of calculations. Since gradient peak capacity is calculated by integrating $1/w(t)$ between t_0 and the retention time of the last eluting compound, t_n , application of Eq. (1.19) requires that t_n be equal to the sum of gradient and hold up times, $t_n = t_0 + t_G$. It ensures that the last compound elutes exactly at the time when the gradient leaves the column. This scenario can be called as an “utterly utilized gradient”. By rearranging Eq. (1.13), t_G can be calculated by the following equation.

$$t_G = k_{\varphi 0} \frac{S t_0 \Delta \varphi}{\exp(S \Delta \varphi) - 1} \quad (1.40)$$

A simple strategy to construct gradient Poppe plot (Listing 1.5) is varying column length in a relatively wide range while particle diameter of the stationary phase, d_p , initial eluent concentration, φ_0 , and the change of eluent composition, $\Delta \varphi$, are set constant. At each column length, the maximal eluent velocity, $u_{0, \max}$, is calculated. It defines the values of plate height, H , and column hold-up time, t_0 . The gradient time, t_G is determined by Eq. (1.40). Finally, the peak capacity of the separation is calculated by Eq. (1.19) at each column length. By plotting the peak time, t_{peak} , against peak capacity, one can construct the gradient Poppe plot. Peak time is the ratio of total analysis time and peak capacity.

$$t_{\text{peak}} = \frac{t_G + t_0}{n} \quad (1.41)$$

```

### Use with Listing 1.1 ###

fi0, dfi = 0.05, 0.7      #initial eluent composition, change of eluent composition
k0, S = 1e6, 20          #parameters of linear solvent strength model, Eq. (1.12)
#retention factor of the last eluting compound at the beginning of analysis
kfi0 = k0*np.exp(-S*fi0)

#-----PLOTTING OF CONSTANT  $t_G+t_0$  LINES-----#
pcs = np.logspace(1,3,10) #definition of range of peak capacities
#iterate through different  $t_0+t_G$  values
for tgt0 in [1e1, 1e2, 1e3, 1e4, 1e5]:
    #at each  $t_0+t_G$ , plot  $(t_0+t_G)/n$  with blue dashed line
    plt.loglog(pcs, tgt0/pcs, 'b--', linewidth=0.5)

#-----CONSTRUCTION OF GRADIENT POPPE CURVES FOR DIFFERENT COLUMN LENGTHS-----#
ls = np.logspace(-3,1,100) #definition of range of column lengths
#iterate through different  $d_p - \Delta P$  data pairs,
# $d_p$  - particle diameter,  $dP$  - max pressure drop,  $c$  - color,  $m$  - linestyle
for dp, dP, c, m in [(1.7e-6, 1200e5, 'C0', '-'), (1.7e-6, 400e5, 'C0', '--'), \
    (3e-6, 600e5, 'C1', '-'), (3e-6, 400e5, 'C1', '--'), (5e-6, 400e5, 'C2', '-')]:
    u0s = dP*dp**2/(fi*eta*ls) #eluent linear velocities
    Hs = h(u0s*dp/dm, A, B, C)*dp #plate heights
    t0s = ls/u0s #column hold-up times
    tgs = kfi0*S*dfi*t0s/(np.exp(S*dfi)-1) #gradient times, see Eq. (1.40)
    pcs = peakcap(tgs, fi0, dfi, t0s, Hs, ls, S, k0) #peak capacities, see Eq. (1.19)
    #plot curves in log-log scale with 'm' linestyle, 'c' color. Add label to legend.
    plt.loglog(pcs, tgs/pcs, m, color=c, \
        label=r'{0:1.1f}  $\mu\text{m}$ , {1:4.0f} bar'.format(dp*1e6, dP*1e-5))

plt.xlim(30, 1000) #set x limits
plt.ylim(0.1,500) #set y limits
plt.xlabel('Gradient peak capacity,  $n$ ') #label of x axis
plt.ylabel(r' $(t_G+t_0)/n$ ') #label of y axis
plt.legend() #show legend
plt.show() #show plot

```

Listing 1.5: Python code for construction of gradient Poppe plot shown in Fig. 1.11.

Note that in the construction of gradient Poppe plot, the column hold-up time should be taken into consideration.

Fig. 1.11 shows gradient Poppe plots of columns operated at different pressures and packed with different particles sizes. For the sake of comparability, the same viscosity and diffusion coefficient were used for the calculations as in Figs. 1.7 and 1.8 even if the applied k_0 (10^6) and S values (20) suggest large molecule, such as large peptide. The trends shown in Fig. 1.11 are similar to the plots in Figs. 1.7. In the practical range of analysis times and column lengths, higher peak capacities can be achieved by using columns packed by smaller particles so long as the maximum operating pressure applicable to the phase is applied. Even if low pressure is used, ultrahigh-performance particles can provide higher rate of peak capacity production and faster analysis than larger particles. The vertical asymptotes of curves presented in Fig. 1.11 correspond to the maximal achievable peak capacities as they are calculated by Eq. (1.22). It can be seen that long columns packed by large particles can provide very high peak capacities, even if it takes high analysis times. The application of large pressures provides higher peak

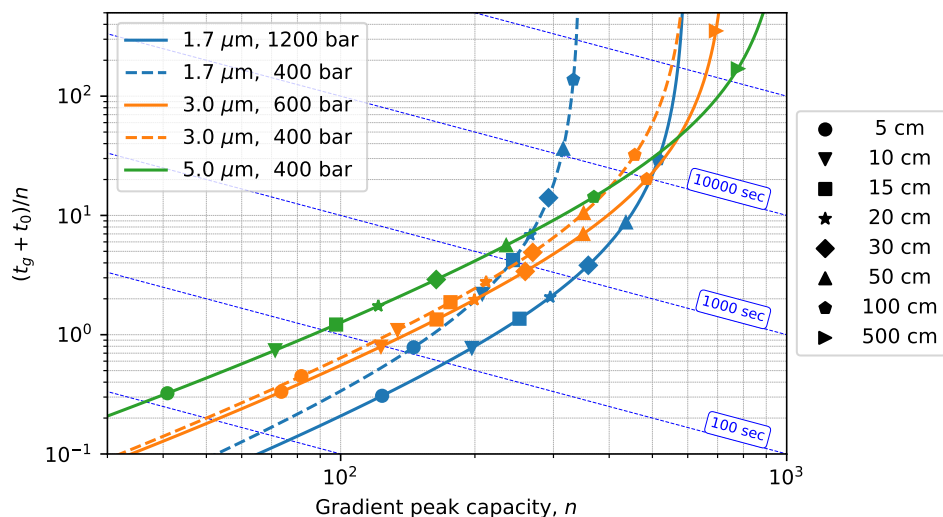


Figure 1.11: Poppe plot of gradient peak capacity for columns operated at different pressures and packed with different particles sizes. Parameters of calculations: $k_0 = 10^6$, $S = 20$, $\varphi = 0.05$, $\Delta\varphi = 0.7$, $D_m = 10^{-9}$ m²/sec, $\eta = 0.001$ Pa sec, $\phi = 1000$.

capacities and faster separations. It is desirable to use a column at the highest applicable flow rate in order to generate the highest peak capacity possible. These conclusions are in agreement with the isocratic Poppe plots.

Comparison of Figs. 1.7 and 1.11 emphasize the obvious conclusion that gradient separations superior over isocratic ones. It was shown that \sqrt{N} in Fig. 1.7 corresponds to the isocratic peak capacity. Therefore, the figures can be compared directly. It can be seen that a ~ 1000 sec separation can generate 200–400 peak capacities in gradient run. The dead-time required to achieve the same order of n in isocratic separation is also ~ 1000 sec. Considering, however, that the total analysis time of an isocratic run is 20–40 times larger than the t_0 when the goal is to reach high separation power, it is indisputable that much higher peak capacities can be generated in much shorter time by gradient separation than by isocratic mode.

Eq. (1.19) shows that gradient steepness, b , is an important factor that influences separation power significantly. b consists of four parameters. S is fixed in the approach used here. t_0 is defined by the column length and pressure drop (through $u_{0,\max}$). The gradient time and change of eluent composition are not mutually independent parameters. Constraint shown in Eq. (1.40) defines their strict relationship. In Fig. 1.11, value of $\Delta\varphi$ was set to 0.7. It is obvious that this artificially chosen parameter cannot serve with the optimal peak capacities and peak times. The proper choice of t_G and $\Delta\varphi$ is essential in the optimization of gradients. Both too steep and too shallow gradients are detrimental to the achievable peak capacity. Therefore, it is necessary to apply an optimization method for the determination of t_G and $\Delta\varphi$.

Fig. 1.12 presents a nomogram-like gradient Poppe plot constructed for 1.7 μm particles,

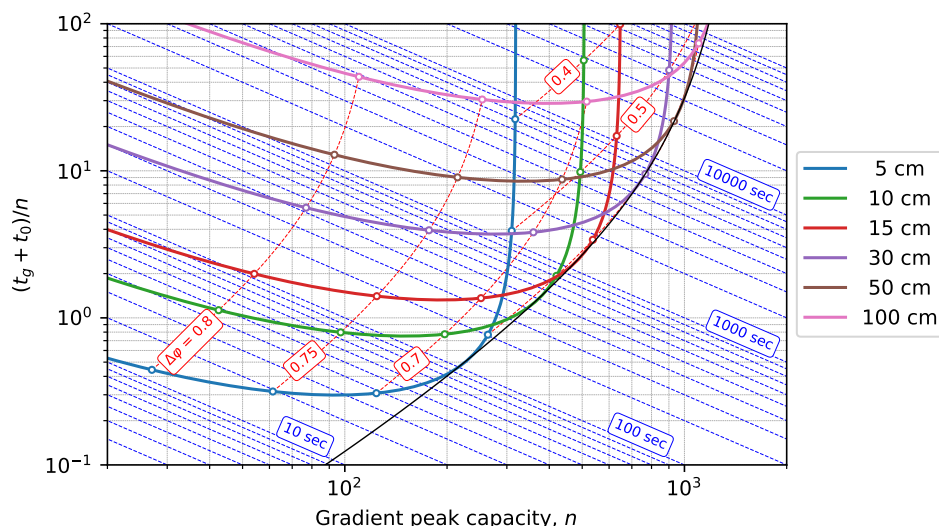


Figure 1.12: Nomogram for the support of optimization of gradient peak separation. For parameters of calculations see Fig. 1.7

1200 bar max. pressure drop, and column lengths that have practical relevance. The figure is similar to Fig. 1.8. It can also be used directly in method development. By using Fig. 1.12, one can find the separation conditions that (1) offer the highest peak capacity in a given analysis time, or (2) requires the shortest time to generate a given peak capacity. In the first case scenario, the analyst should move on the straight line of target analysis time (dashed blue lines on the figure) to find the column length, L , that offer the highest peak capacity. The dead time can be determined from the column length and pressure drop applied in the analysis by rearranging Eq. (1.33) for u_0 . Gradient time, t_G is given as the difference of total analysis time and t_0 . The required change of eluent composition can be determined either by interpolating between the iso- $\Delta\phi$ lines (dashed red lines on the figure), or by calculating it from Eq. (1.40). Since Eq. (1.40) cannot be rearranged to calculate $\Delta\phi$ directly, a proper root finding algorithm, such as the following, is necessary for the calculation of its value:

```
dfi = brentq(lambda dfi: trgrad(tg, fi0, dfi, t0, S, k0)-(t0+tg), 1e-6, 1-fi0)
```

Here we took Brent's method provided by SciPy scientific computing library to find $\Delta\phi$ where the retention time of the last eluting compound is equal to the sum of column hold-up time and gradient time. The bracketing values of $\Delta\phi$ required by Brent's method were chosen as 10^{-6} and $1 - \phi_0$ since $\Delta\phi$ should be larger than zero and smaller than or equal to $1 - \phi_0$.

In the second case scenario, the analyst first should find the column that offer the target peak capacity in the shortest analysis time. It can be determined from Fig. 1.12 directly. The eluent velocity is given by Eq. (1.33). The dead time can be determined as L/u_0 . The total analysis time is given as the product of n and peak time, $(t_G + t_0)/n$. Then, gradient time is given as the difference of total analysis time and t_0 . $\Delta\phi$ can be determined as it was shown in

the first scenario. Alternatively, t_G can be determined by Brent's method after estimating $\Delta\varphi$ from the nomogram:

```
H = h(u0*dp/dm, A, B, C)*dp #calculation of plate height
tg = brentq(lambda tg: peakcap(tg, fi0, dfi, t0, H, L, S, k0)-pctarget, 1e-6, 1e5)
```

Here the Brent's method is used to find t_G that produces the target peak capacity (`pctarget` in the code).

In Fig. 1.12, the thin black envelope shows the overall optimum of gradient separation. The points of envelope represents the optimal column length that produces the highest peak capacity and the lowest peak time at a given analysis time. The envelope demonstrates the limit of achievable separation power by a given type of particle.

Listing 1.6 shows a Python code that allows the construct of nomogram-like Poppe plot for the optimization of gradient separations. In order to be able to construct nomograms such as Fig. 1.12, the analyst has to determine or at least estimate k_0 of the last eluting compound, a nominal S value that represent the overall sample compounds, and the parameters of plate height equation. By generating nomograms like Fig. 1.12 for any phases available in the lab, one can compare different scenarios for the analysis of the given sample. The optimal column dimensions, stationary phases and operating conditions can be determined directly by the use of these nomograms as it was shown in the previous paragraphs.

1.4 Conclusions

Proper optimization of peak capacities of analytical HPLC methods is unavoidable in the analysis of samples containing large number of compounds. A well optimized method can offer the same peak capacity in much less analysis time, consuming much less solvents than a non-optimized procedure. Before any method optimization, the analyst should minimize extra column volumes by changing connection capillaries and detector cell, especially if ultra-high performance columns are used. In this Chapter the construction and application of Poppe plots were demonstrated in analytical method development. Poppe plots are suitable tools in optimization of peak capacities. In isocratic runs, one can optimize the width of retention window and column plate count separately. At the same time, gradient elution needs a holistic optimization. The parameters affecting the peak capacity generated by the chromatographic system are not mutually independent. Change of one parameter changes the optimal value of other parameters as well. Fortunately, Poppe plots offer a general approach for the optimization of both isocratic and gradient separations. By the use of Python codes shared in this chapter, nomograms can be constructed that allow the determination of most of the optimal separation conditions. The use of Poppe plots in method development provide the analyst a simple and effective tool for optimization of HPLC analyses.

```

#-#-#-# Use with Listing 1.1 #-#-#-#

fi0 = 0.05          #initial eluent composition,  $\phi_0$ 
k0, S = 1e6, 20    #parameters of linear solvent strength model
dp, dP = 1.7e-6, 1200e5 #particle diameter and max. pressure drop
#retention factor of the last eluting compound at the beginning of analysis
kfi0 = k0*np.exp(-S*fi0)

#-----CONSTRUCTION OF ISO- $\Delta\phi$  LINES-----#
ls = np.logspace(np.log10(0.05),0,100) #definition of range of column lengths
#iterate through different  $\Delta\phi$  values
for dfi in [0.4, 0.5, 0.6, 0.7, .75, 0.8]:
    u0s = dP*dp**2/(fi*eta*ls) #eluent linear velocities
    Hs = h(u0s*dp/dm, A, B, C)*dp #plate heights
    t0s = ls/u0s #column hold-up times
    tgs = kfi0*S*dfi*t0s/(np.exp(S*dfi)-1) #gradient times, see Eq. (1.40)
    pcs = peakcap(tgs, fi0, dfi, t0s, Hs, ls, S, k0) #peak capacities, see Eq. (1.19)
    plt.loglog(pcs, (tgs+t0s)/pcs, 'r--', linewidth=0.5) #plot iso- $\Delta\phi$  lines in log-log scale

#-----PLOTTING OF CONSTANT  $t_G+t_0$  LINES-----#
pcs = np.logspace(1,3.4,100) #definition of range of peak capacities
#iterate through different  $t_0+t_G$  values
for tgt0 in [1e1, 1e2, 1e3, 1e4, 1e5]:
    #at each  $t_0+t_G$ , plot  $(t_0+t_G)/n$  with blue dashed line
    plt.loglog(pcs, tgt0/pcs, 'b--', linewidth=0.5)

#-----CONSTRUCTION OF GRADIENT POPPE CURVES FOR DIFFERENT COLUMN LENGTHS-----#
dfis = np.linspace(0.05, 1-fi0, 100) #definition of range of column lengths
#iterate through different column lengths that has practical relevance
for length in [0.05, 0.1, 0.15, 0.3, 0.5, 1.0]:
    u0 = dP*dp**2/(fi*eta*length) #eluent linear velocities
    H = h(u0*dp/dm, A, B, C)*dp #plate heights
    t0 = length/u0 #column hold-up times
    tgs = kfi0*S*dfis*t0/(np.exp(S*dfis)-1) #gradient times, see Eq. (1.40)
    pcs = peakcap(tgs, fi0, dfis, t0, H, length, S, k0) #peak capacities, see Eq. (1.19)
    plt.loglog(pcs, (tgs+t0)/pcs) #plot curves in log-log scale

plt.xlim(2e1, 2e3) #set x limits
plt.ylim(1e-1,1e2) #set y limits
plt.xlabel('Gradient peak capacity, $n$') #label of x axis
plt.ylabel(r'$\frac{t_G + t_0}{n}$') #label of y axis
plt.show() #show plot

```

Listing 1.6: Python code for generating nomogram-like gradient Poppe plot.

Acknowledgement

The author acknowledges the financial support of the János Bolyai Research Scholarship of the Hungarian Academy of Sciences.

References

- [1] J. C. Giddings, Maximum number of components resolvable by gel filtration and other elution chromatographic methods, *Anal. Chem.* 39 (1967) 1027–1028.
- [2] U. D. Neue, Peak capacity in unidimensional chromatography, *J. Chromatogr. A* 1184 (2008) 107–130.
- [3] J. W. Dolan, L. R. Snyder, N. M. Djordjevic, D. W. Hill, T. J. Waeghe, Reversed-phase liquid chromatographic separation of complex samples by optimizing temperature and gradient time: I. peak capacity limitations, *J. Chromatogr. A* 857 (1999) 1 – 20.
- [4] J. C. Giddings, Comparison of theoretical limit of separating speed in gas and liquid chromatography, *Anal. Chem.* 37 (1965) 60–63.
- [5] J. H. Knox, M. Saleem, Kinetic conditions for optimum speed and resolution in column chromatography, *J. Chromatogr. Sci.* 7 (1969) 614–622.
- [6] G. Guiochon, Comparison of the theoretical limits of separating speed in liquid and gas chromatography, *Anal. Chem.* 52 (1980) 2002–2008.
- [7] H. Poppe, Some reflections on speed and efficiency of modern chromatographic methods, *J. Chromatogr. A* 778 (1997) 3–21.
- [8] G. Desmet, D. Clicq, P. Gzil, Geometry-independent plate height representation methods for the direct comparison of the kinetic performance of lc supports with a different size or morphology, *Anal. Chem.* 77 (2005) 4058–4070.
- [9] X. Wang, D. R. Stoll, P. W. Carr, P. J. Schoenmakers, A graphical method for understanding the kinetics of peak capacity production in gradient elution liquid chromatography, *J. Chromatogr. A* 1125 (2006) 177–181.
- [10] L. R. Snyder, Linear elution adsorption chromatography. VII. Gradient elution theory, *J. Chromatogr.* 13 (1964) 415–434.
- [11] Cs. Horváth, S. R. Lipsky, Peak capacity in chromatography, *Anal. Chem.* 39 (1967) 1893.

- [12] E. Grushka, Chromatographic peak capacity and the factors influencing it, *Anal. Chem.* 42 (1970) 1142–1147.
- [13] H. Poppe, J. Paanakker, M. Bronckhorst, Peak width in solvent-programmed chromatography. i. general description of peak broadening in solvent-programmed elution, *J. Chromatogr. A* 204 (1981) 77–84.
- [14] L. R. Snyder, D. L. Saunders, Optimized solvent programming for separations of complex samples by liquid-solid adsorption chromatography in columns, *J. Chromatogr. Sci.* 7 (1969) 195–208.
- [15] L. R. Snyder, J. W. Dolan, J. R. Gant, Gradient elution in high-performance liquid chromatography: I. theoretical basis for reversed-phase systems, *J. Chromatogr. A* 165 (1979) 3–30.
- [16] F. Gritti, G. Guiochon, Performance of columns packed with the new shell kinetex-c18 particles in gradient elution chromatography, *J. Chromatogr. A* 1217 (2010) 1604–1615.
- [17] F. Gritti, C. A. Sanchez, T. Farkas, G. Guiochon, Achieving the full performance of highly efficient columns by optimizing conventional benchmark high-performance liquid chromatography instruments, *J. Chromatogr. A* 1217 (2010) 3000–3012.
- [18] S. Fekete, J. Fekete, The impact of extra-column band broadening on the chromatographic efficiency of 5cm long narrow-bore very efficient columns, *J. Chromatogr. A* 1218 (2011) 5286–5291.
- [19] L. R. Snyder, J. J. Kirkland, J. W. Dolan, *Introduction to Modern Liquid Chromatography*, John Wiley & Sons, Inc., 2010.
- [20] K. Horváth, F. Gritti, J. N. Fairchild, G. Guiochon, On the optimization of the shell thickness of superficially porous particles, *J. Chromatogr. A* 1217 (2010) 6373–6381.
- [21] T. J. Causon, E. F. Hilder, R. A. Shellie, P. R. Haddad, Probing the kinetic performance limits for ion chromatography. ii. gradient conditions for small ions, *J. Chromatogr. A* 1217 (2010) 5063–5068.
- [22] X. Wang, W. E. Barber, W. J. Long, Applications of superficially porous particles: High speed, high efficiency or both?, *J. Chromatogr. A* 1228 (2012) 72–88.
- [23] S. Fekete, D. Guillarme, Possibilities of new generation columns packed with 1.3 μ m core-shell particles in gradient elution mode, *J. Chromatogr. A* 1320 (2013) 86–95.

- [24] S. Fekete, J.-L. Veuthey, D. Guillarme, Achievable separation performance and analysis time in current liquid chromatographic practice for monoclonal antibody separations, *J. Pharmaceut. Biomed.* 141 (2017) 59–69.